

FIRST-PRINCIPLES CALCULATION OF THE STRUCTURE OF MERCURY

MICHAEL J. MEHL

Complex Systems Theory Branch, Naval Research Laboratory, Washington, DC 20375-5345

ABSTRACT: Mercury has perhaps the strangest behavior of any of the metals. Although the other metals in column IIB have an *hcp* ground state, mercury's ground state is the body centered tetragonal β Hg phase. The most common phase of mercury is the rhombohedral α Hg phase, which is stable from 79K to the melting point and meta-stable below 79K. Another rhombohedral phase, γ Hg, is believed to exist at low temperatures. First-principles calculations are used to study the energetics of the various phases of mercury. Even when partial spin-orbit effects are included, the calculations indicate that the hexagonal close packed structure is the ground state. It is suggested that a better treatment of the spin-orbit interaction might alter this result.

INTRODUCTION

Of all the metals in the periodic table, mercury has the most interesting behavior. A liquid at room temperature, the metal only solidifies below 234K. This phase, denoted α Hg, (Pearson symbol hR1, space group $R\bar{6}m$, *Strukturbericht* designation A10), is a rhombohedral structure with one atom per unit cell and the primitive vectors at an angle of $70^\circ 44.6'$ [1]. Although α Hg has been seen experimentally down to 5K, below 79K the ground state is the phase β Hg (prototype α Pa, Pearson symbol tI2, space group I4/mmm, *Strukturbericht* designation A_a), a body-centered tetragonal (*bct*) phase with a c/a ratio of 0.7071[2]. Nearer to room temperature, α Hg can be transformed to β Hg by applying pressure. A third, meta-stable form, γ Hg, has also been observed[2]. Like α Hg it is rhombohedral with one atom per unit cell, but the primitive vectors are at an angle of about 50° .

Since these phases of mercury all involve only one atom per unit cell, first-principles *ab initio* methods are relatively easy to use. An extensive literature search, however, found very few studies of mercury[5, 6, 7], with only one [7] including relativistic effects, which are important for all of the late fifth-row elements, and that only for metallic clusters. It is useful, therefore, to perform a series of first-principles calculations for the various phases of mercury. This paper presents results using the full potential, Linearized Augmented Plane Wave (LAPW) method[8, 9, 10] using the Hedin-Lundqvist[11] parametrization of the Local Density Approximation (LDA)[12] to Density Functional Theory (DFT)[12, 13]. The calculations were initially performed in the scalar-relativistic approximation[14], which essentially ignores the spin-orbit interaction while maintaining the remaining relativistic contributions. Spin-orbit corrections were then included using the “second-variational” method[15].

THE STRUCTURES OF MERCURY

The primary structures of mercury are the rhombohedral α Hg phase and the body-centered tetragonal β Hg phase. Each phase can be described by two parameters: the volume and a parameter describing the orientation of the primitive vectors. In α Hg this parameter is the angle α between the primitive vectors. In β Hg the parameter is the c/a

ratio of the tetragonal unit cell. Special values of these parameters lead to higher symmetry unit cells. The primitive vectors of the rhombohedral α Hg phase can be written in the form

$$\begin{aligned}\mathbf{a}_1 &= a (1 + x, x, x) \\ \mathbf{a}_2 &= a (x, 1 + x, x), x = \frac{1}{3}(\sqrt{(1 + 2 \cos \alpha)/(1 - \cos \alpha)} - 1) \\ \mathbf{a}_3 &= a (x, x, 1 + x)\end{aligned}\quad (1)$$

where α is the angle between the primitive vectors. There are several special values of this angle. At $\alpha = 0$ the vectors (1) are collinear, while at $\alpha = 2\pi/3$ they are coplanar. These unphysical situations bound the range of α . Several high symmetry lattices can also be obtained from (1). At $\alpha = \pi/3$ we find the *fcc* lattice, at $\alpha = \pi/2$ the simple cubic (*sc*) lattice, and at $\cos \alpha = -1/3$ the *bcc* lattice. Because of these symmetries, a plot of the energy $E(V, \alpha)$ at fixed volume V would show the energy diverging as α approached both zero and $2\pi/3$, with extremal points at $\alpha = \pi/3, \pi/2$, and $\cos^{-1}(-1/3)$. Since the α Hg phase has $\alpha \approx 70^\circ$ degrees, this phase will appear between the *fcc* and *sc* phases. The γ Hg phase, with $\alpha \approx 50^\circ$, has a smaller angle than the *fcc* phase. Figure 1 shows several of the phases found in the rhombohedral system.

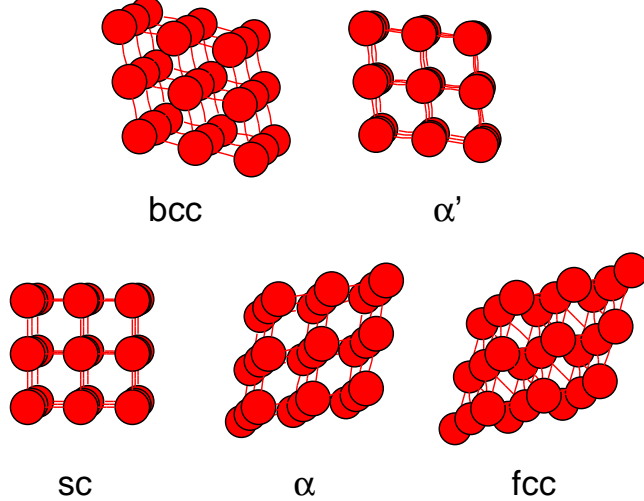


Figure 1: Several of the structures found in the rhombohedral system. The α' phase shown here has an angle α between $\pi/2$ and $\cos^{-1}(-1/3)$. The γ Hg phase would be to the right of the *fcc* phase in this plot.

The primitive vectors of the *bct* β Hg phase can be written in the form

$$\begin{aligned}\mathbf{a}_1 &= (a, 0, 0) \\ \mathbf{a}_2 &= (0, a, 0) \\ \mathbf{a}_3 &= (\frac{1}{2}a, \frac{1}{2}a, \frac{1}{2}c)\end{aligned}\quad (2)$$

This lattice is identical to the *fcc* lattice when $c/a = \sqrt{2}$, and to the *bcc* lattice when $c/a = 1$. It is interesting to note that, within experimental error, the β Hg lattice has $c/a = 1/\sqrt{2}$. At this value of c/a each mercury atom has two nearest neighbors, located directly above and below the atom along the z axis, at $\pm(2\mathbf{a}_3 - \mathbf{a}_1 - \mathbf{a}_2)$, and eight next-nearest neighbors. The mercury atoms thus form chains running along the z direction. Figure 2 shows several phases in the *bct* system.

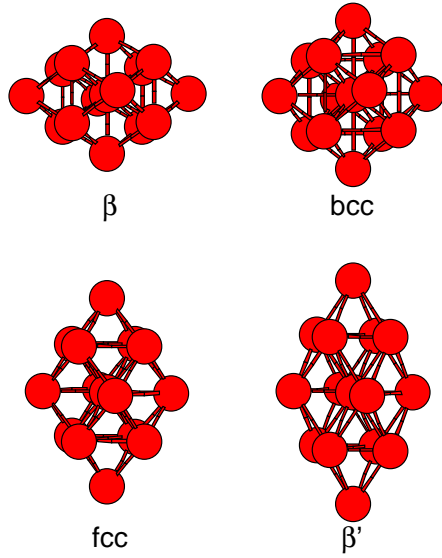


Figure 2: Several of the structures found in the *bct* system². The β' phase shown here has a value of c/a between the *fcc* and *bcc* phases.

FIRST-PRINCIPLES CALCULATIONS

The first set of calculations were performed using the LAPW method in the “scalar-relativistic” approximation outlined above. This method essentially ignores the spin-orbit interaction, keeping the remainder of the relativistic corrections. In all of the calculations the muffin-tin radius was set at $R_{MT} = 2.2$ atomic units, a size chosen to allow large strains of the form (1) or (2) while keeping the muffin tins from touching. The momentum cutoff K_{max} was chosen so that $R_{MT}K_{max} = 10.5$, yielding typical secular-equation dimensions of about 300×300 . Increasing the cutoff to 11.5 decreases the energy by about 0.3 m Ry for all structures and volumes. The K-point meshes were chosen using a regular mesh evenly spaced along the primitive vectors. Meshes of 150-200 K-points in the irreducible Brillouin zone, depending on the structure, yield total energies accurate to about 0.3 mRy compared to larger K-point meshes. The energies computed here are thus accurate to about 0.5 mRy.

Comparing the scalar-relativistic and spin-orbit energies obtained from a Liberman-based atomic code[16] show that the spin-orbit interaction contributes 29.5 mRy to the total energy. This is a relatively large contribution, so the spin-orbit interaction is included by a variational method[15]. The spin-orbit energy is essentially converged if the second-variational basis uses 30 LAPW eigenstates in the variational calculation.

Energy-volume curves were calculated for mercury in the *fcc*, *bcc* and *sc* cubic lattices, the hexagonal close packed (*hcp*) lattice, and the lattices described by (1) and (2) above. For convenience the latter structures will be referred to as α Hg and β Hg, even when they are outside the range of parameters which properly describe these structures. While the cubic structures require only knowledge of the volume to determine the structural energy, the *hcp*, α Hg, and β Hg structures, require a knowledge of the energy as a function of the other lattice parameter. For the *hcp* and β Hg phases this parameter is c/a , while for α Hg it is the angle α described in (1). Calculations were performed in both the scalar-relativistic approximation and with the variational spin-orbit energy included.

The computations for α Hg are shown in Figure 3. At most volumes there are two

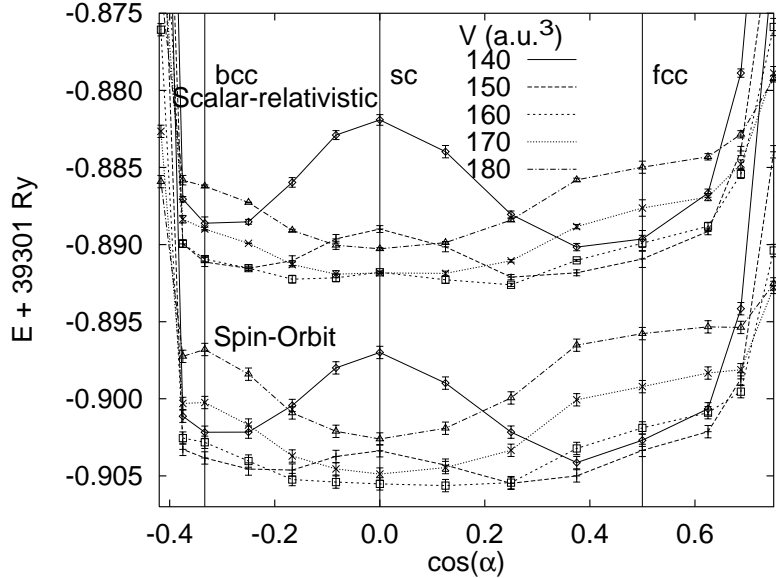


Figure 3: LAPW calculation of the total energy of α Hg in the rhombohedral structure (system1). Both scalar-relativistic and spin-orbit results are shown. The error bars represent the estimated uncertainties in the energies. The lines between the points are drawn as an aid to the eye.

minima in this plot, the global minimum between the *sc* and *fcc* structures, corresponding to the observed α Hg phase, and a secondary minimum between the *bcc* and *sc* structures, which will be denoted α' Hg. These minima coalesce to the *sc* structure at large volumes. There are no minima in the region of the γ Hg phase[2]. Since this phase was obtained by shearing α Hg, it is possible that the phase is stabilized by a non-hydrostatic shear.

Similar calculations for β Hg are presented in Figure 4. Again, there are two minima. The first, corresponding to the observed β Hg structure, is near $c/a \approx 0.7$. The second, denoted β' Hg, has a rather large shear of $c/a \approx 1.7$. This is analogous to the large c/a ratio found in the *hcp* structures of Zn and Cd, and to the c/a ratio found in the calculations for *hcp* Hg. Note that without the spin-orbit interaction the β' Hg phase is lower in energy than the β Hg phase, but the energy difference is not significant. The spin-orbit interaction lowers the energy of the β Hg phase so that it is favored over the β' Hg phase.

The energy-volume curves for the low energy structures of mercury are calculated by finding the minimum energy as a function of the strain lattice parameter at each volume for the α Hg, β Hg, and *hcp* Hg structures. The equilibrium energies for each of these phases is shown in Table I, and the full energy volume curves are shown in Figure 5. From the calculations we must conclude that the *hcp* structure is the ground state of mercury, contrary to experiment. The spin-orbit interaction does not change the relative ordering of the phases, and differences in the value of the spin-orbit interaction (the Δ column in Table I) are numerically insignificant. In addition, we see that the total energy calculations cannot distinguish between the α Hg and the α' Hg phases, nor between the β Hg and the β' Hg phases.

If we nevertheless restrict ourselves to looking at the experimentally observed phases, we find the structural properties are in good agreement with experiment (Table II). The calculated volume of the α Hg phase is about 13% smaller than the experimental volume,

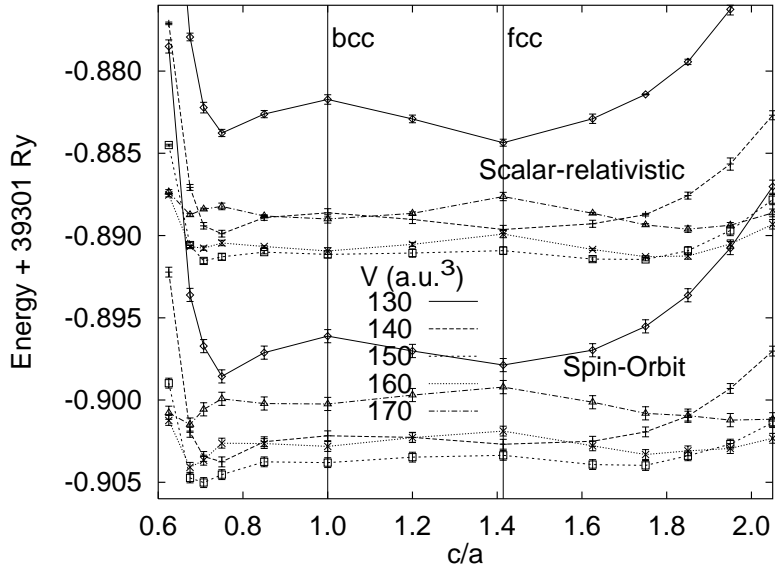


Figure 4: LAPW calculation of the total energy of β Hg in the *bct* structure (system2). Both scalar-relativistic and spin-orbit results are shown. The error bars represent the estimated uncertainties in the energies. The lines between the points are drawn as an aid to the eye.

while the β Hg phase is only 1% smaller than the experimental volume. These results are consistent with LDA calculations for similar structures. The calculations do overestimate the angle (α) for the α Hg phase, but get the c/a ratio correctly in the β Hg phase.

DISCUSSION

Given the many successes of the DFT, and LDA in particular, in determining the structural properties of crystals, it is somewhat disturbing that we cannot correctly predict the ordering of the low-lying energy states of mercury. There are, of course, possible improvements to the LDA[17], and these may provide part of the answer. A more obvious problem with the present calculation is the form of the spin-orbit calculation. The present method[10, 15] uses scalar-relativistic orbitals as a basis for the second diagonalization of the Hamiltonian including the spin-orbit interaction. This is a good basis set for most states, but it has serious difficulties in dealing with the p states, since the relativistic $p_{1/2}$

Table I: The equilibrium energies for several structures of mercury, shifted so that the energy of the scalar-relativistic *hcp* phase is set to zero. The second column shows the scalar-relativistic energy, the third the energy including the spin-orbit interaction, and the fourth the difference between the two. The “primed” phases are defined in the text. The energy of atomic Hg is also shown.

Phase	Scalar	Spin-Orbit	Δ	Phase	Scalar	Spin-Orbit	Δ
<i>fcc</i>	.00244	-.01013	.01257	α	.00092	-.01230	.01322
<i>bcc</i>	.00219	-.01010	.01229	α'	.00131	-.01237	.01368
<i>sc</i>	.00139	-.01200	.01339	β	.00196	-.01160	.01356
<i>hcp</i>	.00000	-.01309	.01309	β'	.00193	-.01096	.01289
atom	.02947	-.00466	.02947				

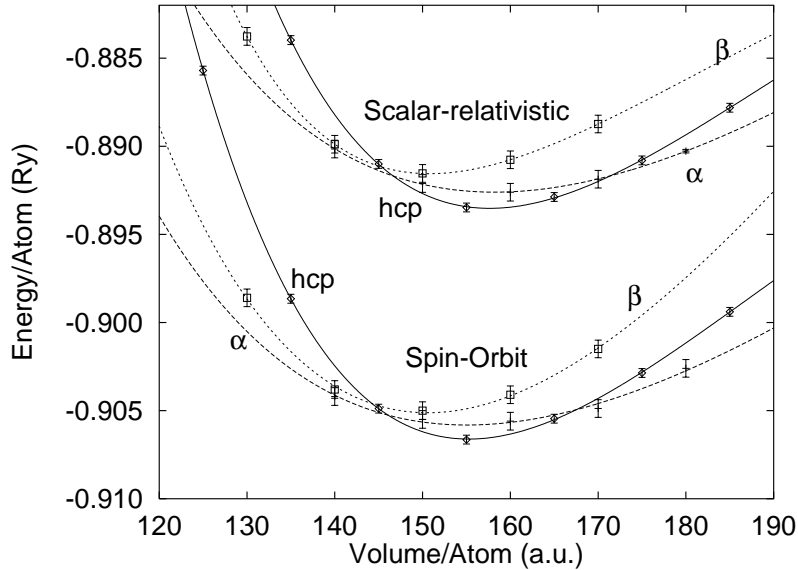


Figure 5: LAPW calculation of the total energy Hg as a function of volume for the α Hg, β Hg, and *hcp* phases. Both scalar-relativistic and spin-orbit results are shown. The error bars represent the estimated uncertainties in the energies. The lines between the points represent a Birch fit to the points shown.

state is non-zero at the origin, while the scalar-relativistic p state vanishes there. This leads to an underestimation of the spin-orbit interaction of about 50% in this case, as can be seen in Table I. In the atomic calculation, where it is calculated exactly, the spin-orbit interaction contributes 29.5 mRy to the total energy. For the bulk structures, however, where the spin-orbit interaction is only approximated, it contributes about 13 mRy/atom to the total energy. It seems likely that a better treatment of the spin-orbit interaction will increase this contribution. It has been suggested[10] that inclusion of $p_{1/2}$ -like local orbitals in the LAPW basis would improve the spin-orbit energy, but this suggestion has yet to be implemented.

ACKNOWLEDGMENTS

Partial support for this work was provided by the US Office of Naval Research. I also wish to thank David Singh for useful discussions concerning the spin-orbit corrections, and Larry Boyer for discussions concerning the “magic strains”.

Table II: Structural properties of the α Hg and β Hg phases obtained from the LAPW calculations described in the text, compared to experiment.

	α Hg			β Hg			
	V (a.u. ³)	a (a.u.)	α (deg)	V (a.u. ³)	a (a.u.)	c (a.u.)	c/a
Experiment	179.7	5.643	70.743	152.1	7.549	5.338	0.7071
Scalar-relativistic	158.2	5.408	75.6	150.8	7.52	5.34	0.71
Spin-Orbit	155.0	5.372	80.2	150.6	7.52	5.33	0.71

References

- [1] R. W. G. Wycoff, Crystal Structures Vol. 1, 2nd edition, (John Wiley and Sons, New York, 1963), pp. 17-18.
- [2] J. Donohue, The Structures of the Elements, (John Wiley & Sons, New York, 1974), pp. 191-199.
- [3] L. L. Boyer, *Acta Crystallogr. A* **45**, FC29 (1989).
- [4] E. C. Bain, *Trans. AIME*, **70**, 25 (1924).
- [5] P. Ballone and G. Galli, *Phys. Rev. B* **40**, 8563 (1989).
- [6] P. Neisler and K. S. Pitzer, *J. Phys. Chem.* **91**, 1084 (1987).
- [7] P. P. Singh, *Phys. Rev. B* **49**, 4954 (1994).
- [8] O.K. Andersen, *Phys. Rev. B* **12** 3060 (1975)
- [9] S.H. Wei and H. Krakauer, *Phys. Rev. Lett.* **55** 1200 (1985).
- [10] D. J. Singh, Planewaves, Pseudopotentials, and the LAPW Method, (Kluwer Academic Publishers, Boston, 1994).
- [11] L. Hedin and B. I. Lundqvist, *J. Phys. C* **4**, 2064 (1971).
- [12] W. Kohn and L.J. Sham, *Phys. Rev.* **140** A1133 (1965).
- [13] P. Hohenberg and W. Kohn, *Phys. Rev.* **136**, B864 (1964).
- [14] D. D. Koelling and B. N. Harmon, *J. Phys. C* **10**, 2041 (1975).
- [15] A. H. MacDonald, W. E. Pickett, and D. D. Koelling, *J. Phys. C* **13**, 2675 (1980).
- [16] D. A. Liberman, D. T. Cromer, and J. J. Waber, *Comput. Phys. Commun.* **2**, 107 (1971).
- [17] J. P. Perdew, J. A. Chevary, S. H. Vosko, K. A. Jackson, M. R. Pederson, D. J. Singh, and C. Fiolhais, *Phys. Rev. B* **46**, 6671 (1992) and references therein.